Soft Matter

PAPER

View Article Online
View Journal | View Issue

Cite this: *Soft Matter*, 2020, **16**, 3029

Effects of topological constraints on linked ring polymers in solvents of varying quality

Zahra Ahmadian Dehaghani, [a] Iurii Chubak, [b] Christos N. Likos *[b] and Mohammad Reza Ejtehadi *[ac]

Received 2nd December 2019,
Accepted 20th February 2020

DOI: 10.1039/c9sm02374g

rsc.li/soft-matter-journal

We investigate the effects of topological constraints in catenanes composed of interlinked ring polymers on their size in a good solvent as well as on the location of their θ-point when the solvent quality is worsened. We mainly focus on poly[*n*]catenanes consisting of n ring polymers each of length m interlocked in a linear fashion. Using molecular dynamics simulations, we study the scaling of the poly[*n*]catenane's radius of gyration in a good solvent, assuming in general that $R_g \sim m^{\mu}n^{\nu}$ and we find that $\mu = 0.65 \pm 0.02$ and $\nu = 0.60 \pm 0.01$ for the range of n and m considered. These findings are further rationalized with the help of a mean-field Flory-like theory yielding the values of $\mu = 16/25$ and $\nu = 3/5$, consistent with the numerical results. We show that individual rings within catenanes feature a surplus swelling due to the presence of N_L topological links. Furthermore, we consider poly[*n*]catenanes in solvents of varying quality and we demonstrate that the presence of topological links leads to an increase of its θ-temperature in comparison to isolated linear and ring chains with the following ordering: $T^{\theta}_{\text{catenane}} > T^{\theta}_{\text{linear}} > T^{\theta}_{\text{ring}}$. Finally, we show that the presence of links similarly raises the θ-temperature of a single linked ring in comparison to an unlinked one, bringing its θ-temperature close to the one of a poly[*n*]catenane.

1 Introduction

Molecular topology of polymers has a pronounced effect on their in- and out-of-equilibrium behavior in melts and solutions. The simplest manifestations of a topologically nontrivial state are ring or circular polymers, which can be obtained by linking together the ends of an ordinary linear chain. In fact, such a seemingly straightforward concatenation operation dramatically reduces the number of attainable states in the phase space, resulting in an effective topological repulsion between rings[1–6] and, therefore, in far-reaching implications for the static and dynamic properties of the systems thereof. Many remarkable and unique features of ring polymers have been revealed only very recently. For instance, it has been shown that entangled ring polymer melts show an unusual power-law stress relaxation[7] and exhibit crumpled globule conformations in equilibrium that are very distinct from the ones of entangled linear polymer melts.[8–10] Furthermore, it has been conjectured that concentrated solutions or melts of very long rings can undergo a glass transition purely on the basis of topological interactions,[11,12] highly likely due to extensive inter-ring threading,[13,14] whereas recently it has been shown that the glass transition can be triggered by the enhanced segmental activity for the rings of moderate lengths.[15] Finally, even dilute systems of rings feature intriguing properties ranging from a lower θ-temperature of ring polymers in solution[16,17] to enhanced propensity of rings to structure in confinement[18,19] as well as their behavior in microfluidic flows,[20–22] which is clearly distinct from that of linear chains.

Circular DNAs that can be found in viruses and bacteria serve as a good example of natural ring polymers. As a semi-flexible polymer, DNA features interesting behavior due to its elasticity and bending properties,[23–25] especially in the cyclization process, during which a linear DNA chain turns into a cyclic one.[26,27] Even more intriguing phenomena, such as supercoiling,[28,29] can be observed in various types of DNA topologies. Less studied topological structures of circular DNA are mechanically interlocked architectures. Over the last few decades, these structures that are mainly composed of mechanically interlocked ring molecules (macrocycles), such as polycatenanes,[30] have been synthesized[31–33] and observed *in vivo*.[34,35] These macromolecular structures can be potentially utilized in artificial molecular machines[36] and drug delivery systems.[37] The order in which macrocycles are connected to each other leads to various concatenation scenarios.[38] The simplest possible

[a] *Department of Physics, Sharif University of Technology, P. O. Box 11155-9161, Tehran, Iran. E-mail: ejtehadi@sharif.edu*
[b] *Faculty of Physics, University of Vienna, Boltzmanngasse 5, A-1090 Vienna, Austria. E-mail: christos.likos@univie.ac.at*
[c] *School of Nano-Science, Institute for Research in Fundamental Sciences (IPM), P.O. Box 19395-5531, Tehran, Iran*

structure, a [2]catenane, contains two interlocked ring polymers (that is, a Hopf link[38]), whereas connecting n rings ($n \geq 3$) in linear, branched (also star-shaped) or cyclic fashion yields [n]catenanes of the corresponding architecture. Furthermore, interlocking a large number of rings in a random way results in a catenane network,[39,40] better known as an olympic gel.[41,42] Among the above-listed classes of catenanes, [2]catenanes have been widely studied by means of experimental[38,43–45] and computational[46–50] methods due to their relative simplicity. In contrast, poly[n]catenanes, that is linear sequences of n monodisperse interlocked ring chains, with potentially much richer bulk behavior[33] have been investigated much less,[33,51–53] mainly due to major challenges in their synthesis.[33,54–58] The longest up-to-date poly[n]catenane, which has been synthesized only very recently,[33] contains $n = 26$ macrocycles.

Despite advances in developing efficient synthesis protocols for oligo and poly[n]catenanes, from the point of view of polymer physics not much is known about their static and dynamic single-molecule properties, let alone their collective behavior and rheological response. Pakula and Jeszka[51] have used a cooperative motion algorithm on a lattice to study static and dynamic properties of isolated poly[n]catenanes. Their results suggest that the size scaling of large enough poly[n]catenanes in a good solvent is generally similar to that of linear polymers with the equivalent number of monomers (featuring same exponents) and that the relaxation of isolated poly[n]catenanes is slower than the one of isolated linear and ring polymer chains. More recently, Rauscher *et al.*[53] have employed off-lattice molecular dynamics (MD) simulations and a Rouse mode analysis to study the dynamics of isolated poly[n]catenanes and they have shown that due to mechanical bonds, the dynamics is considerably slowed down at short length scales, although the large length scale relaxation is not reduced much in comparison to isolated linear polymers. In contrast to usual covalently bonded polymeric chains, the ''monomers'' of a catenane are themselves short or moderately long macromolecules, also called macrocycles, that are held together by means of topological uncrossability constraints. Such topological (or mechanical) bonds locally enhance two-body contacts between Kuhn segments of neighboring macrocycles. In principle, this irreversible topological, as opposed to covalent, linking between the macromolecular, cyclic ''monomers'' of the poly[n]catenane, can have quantitative effects on single-molecule scaling relations for the size of the catenane under good solvent conditions as well as on the location of its θ-temperature, as compared to linear and ring chains, upon worsening the solvent quality. Furthermore, it is highly likely that such enhanced two-body interactions will affect the properties of macrocycles within a catenane alone and that they will depend on the number N_L piercings a given macrocycle experiences with other macrocycles, as present, for example, in star-shaped catenane structures.

In this article, we aim at exploring these effects employing MD simulations, outlined in Section 2. The rest of the article is structured as follows. In Section 3, we investigate the scaling of the radius of gyration R_g of an isolated poly[n]catenane composed of n rings each of length m with n and m independently under good solvent conditions, supplementing it with mean-field, Flory-like arguments.[59] In Section 4, we consider poly[n]catenanes in solvents of varying quality and the effect of topological bonds on their θ-temperature. Subsequently, in Section 5 we look into the properties of individual macrocycles within a catenane by examining its swelling due to the links with N_L other macrocycles in a good solvent as well as the effect of such topologically restricted conditions on the macrocycle's θ-point. Finally, in Section 6 we summarize and draw our conclusions.

2 Model and methods

We employed for all polymer architectures considered in this work, that is for linear, ring, poly[n]catenanes, as well as star-shaped catenanes, a single coarse-grained model that implicitly takes into account varying quality of the solvent. In particular, we model solvent-dependent attractions between monomers of a macromolecule by means of a Lennard-Jones potential with variable depth:[60]

$$U_{LJ}(r) = \begin{cases} 4\varepsilon\left[\left(\frac{\sigma}{r}\right)^{12} - \left(\frac{\sigma}{r}\right)^{6}\right] + \varepsilon(1-\lambda), & r \leq 2^{1/6}\sigma, \\ 4\varepsilon\lambda\left[\left(\frac{\sigma}{r}\right)^{12} - \left(\frac{\sigma}{r}\right)^{6}\right], & r > 2^{1/6}\sigma, \end{cases} \quad (1)$$

where σ is the steric diameter of each monomer, ε sets the energy scale, and we use the dimensionless coupling parameter λ to control the depth of the potential well. Setting $\lambda = 0$ in eqn (1) makes the monomer–monomer interaction purely repulsive, hence mimicking good solvent conditions, whereas increasing λ induces attractions between monomers and therefore can be associated with worsening of the solvent quality ($\lambda = 1$ is the standard Lennard-Jones potential). For computational efficiency, the potential (1) was truncated and shifted at $r_{cut} = 3\sigma$ for all $\lambda \neq 0$ (for $\lambda = 0$, $r_{cut} = 2^{1/6}\sigma$).

The connectivity between covalently-bound monomers was maintained *via* a harmonic potential:

$$U_{bond}(r) = \frac{K(r - r_0)^2}{2}, \quad (2)$$

with the equilibrium bond length $r_0 = \sigma$ and the spring constant $K = 1000\varepsilon$. Such a moderately high value of K in conjunction with hard-core excluded volume interactions (1) renders the bonds essentially uncrossable, hereby capable of preserving mechanical interconnections in catenanes and avoiding any topological changes in general.

The bending rigidity of the macrocycles was included by means of a harmonic angle potential:

$$U_{bend}(\theta) = \frac{K_\theta(\theta - \theta_0)^2}{2}, \quad (3)$$

where θ is the angle between two neighboring bond vectors in a ring, the bending constant has the value $K_\theta = 4\varepsilon$ and the rest angle $\theta_0 = \pi$. Such a choice of K_θ corresponds to semi-flexible

segments with Kuhn length $l_k \approx 8\sigma$, which was computed from the expectation value $\langle \cos\alpha \rangle = \exp(-s/l_k)$ for a linear polymer with α denoting the angle between the bond vectors $\mathbf{b}_1 = \mathbf{r}_2 - \mathbf{r}_1$ and $\mathbf{b}_s = \mathbf{r}_{s+1} - \mathbf{r}_s$. In addition, where explicitly mentioned, we simulated fully flexible polymer chains with $K_\theta = 0$.

We performed MD simulations in the *NVT* ensemble at a reduced temperature $k_B T/\varepsilon = 0.8$ using the large-scale atomic/molecular massively parallel simulator (LAMMPS)[61] and the HOOMD-blue simulation package.[62–64] The mass of each bead m, its size σ, and the energy ε were chosen as fundamental units. The equations of motion were integrated with the time step $\Delta t = 0.005\tau$, where $\tau = \sigma(m/\varepsilon)^{1/2}$.

Here and in what follows, we use the notation of Rauscher *et al.*,[53] where n stands for the number of macrocycles in a poly[n]catenane, m denotes the polymerization degree of a macrocycle itself, whereas the total polymerization degree of the macromolecule is $N = n \times m$. Such a notation implies that for an isolated ring $N = m$. Furthermore, we will interchangeably refer to the constituents of a catenane as to "macrocycles" or "rings". To characterize the polymer's size, we compute its root mean square radius of gyration, which reads as

$$R_g \equiv \langle R_g^2 \rangle^{1/2} = \left\langle \frac{1}{N} \sum_{i=1}^{N} (\mathbf{r}_i - \mathbf{r}_{CM})^2 \right\rangle^{1/2} \quad (4)$$

with $\mathbf{r}_i$ denoting the position of the i-th monomer in the polymer, $\mathbf{r}_{CM}$ being the position of its center of mass, and the angles $\langle \cdots \rangle$ standing for a statistical average. To avoid potential confusion, hereafter the upper case R_g denotes the radius of gyration of catenanes, whereas the lower case r_g refers to the radius of gyration of individual ring or linear polymer chains, as well as to that of macrocycles within a catenane.

3 Scaling relations for poly[*n*]catenanes in a good solvent

As stated above, poly[n]catenanes are linear chains of mechanically interlocked ring polymers. Looking at the catenanes at a length scale comparable to the size of a single constituent ring, it is reasonable to assume that the macromolecule is a simple linear chain with a polymerization degree n composed of topologically bonded "macromonomers" of length m. Given this representation, the size R of a catenane under good and athermal solvent conditions is approximately $R \approx bn^\nu$, where b stands for the size of an individual "macromonomer" and the exponent ν assumes the self-avoiding random walk value[59] $\nu_0 = 0.588 \approx 3/5$. Furthermore, since the monomeric units within a catenane are polymers themselves, their size b in a good solvent can be equivalently expressed as $b \approx b_0 m^\mu$, where the constant b_0 is comparable to the size of a microscopic chemical monomer and μ again equals to ν_0. As a result, the total size

$$R \approx b_0 (mn)^{\nu_0} \quad (5)$$

and therefore $R \sim N^{3/5}$, which is in full agreement with the result for linear polymer chains of the respective length N in a good solvent. The preceding argumentation offers a straightforward way of estimating the size of a catenane, except that it might not be entirely true. As will be shown below, in comparison to (5) a more generic relation appears to hold, where the total size R scales with n and m as

$$R \approx b_0 m^\mu n^\nu, \quad (6)$$

where $\nu = \nu_0$ and the exponent μ governing the scaling of R with respect to the macrocycle's size is different from ν and exceeds it by about 10%.

To verify the scaling relation (6) and to determine the exponents μ and ν, we systematically simulated an ensemble of isolated poly[n]catenanes that are composed of n (n = 1, 2, 4, 8, 16, 32 and 64) interlocked ring polymers of various lengths m (m = 10, 16, 32, 64, 128 and 256). The biggest catenane contained N = 16 384 beads corresponding to m = 256 and n = 64. Here, we investigate semi-flexible polymer chains with the bending constant $K_\theta = 4\varepsilon$ under good solvent conditions, $\lambda = 0$ in eqn (1), to evoke comparison with the poly[n]catenanes that have been synthesized experimentally.[33] A representative conformation of a simulated poly[n]catenane is shown in Fig. 1. To determine the exponents μ and ν in the ansatz (6), we plot the radii of gyration of poly[n]catenanes as a function of m for different fixed values of n and as a function of n for different fixed values of m in Fig. 2(a) and (b), respectively. The mean radii of gyration of each poly[n]catenane used in Fig. 2 were averaged over at least 5 ($n \leq 8$) and 10 ($n > 8$) independent simulation runs of total length $\mathscr{T} = 10^6 - 10^7\tau$ and the corresponding error bars are smaller than the symbol sizes. To ensure statistical significance, more independent runs starting from different initial configurations were used for the biggest catenanes considered (n = 32, 64 with N = 128, 256) as their conformational relaxation is much slower compared to shorter macromolecules.

The exponents μ and ν were obtained by fitting R_g of a poly[n]catenane using the expressions $R_g(m) = Am^\mu$ (for a fixed n) and $R_g(n) = Bn^\nu$ (for a fixed m), respectively, with the first few initial values of R_g discarded in both cases (A, B are fitting parameters). The dashed gray lines in Fig. 2(a) and (b) indicate the obtained fits and the resulting values of μ and ν are given in Fig. 2(c) and (d), respectively. First of all, for a single

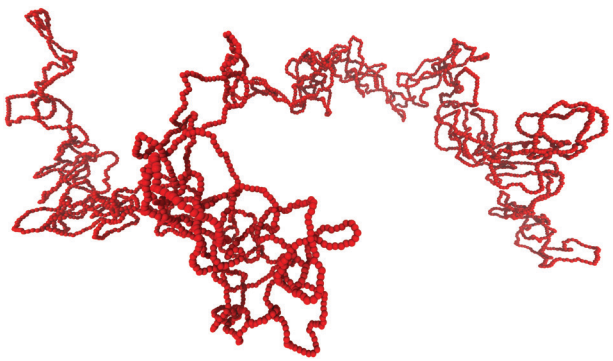

Fig. 1 Snapshot from a simulation of a semi-flexible ($K_\theta = 4\varepsilon$) poly[n]-catenane composed of n = 64 macrocycles linked in a linear fashion each of size m = 64 under good solvent conditions.

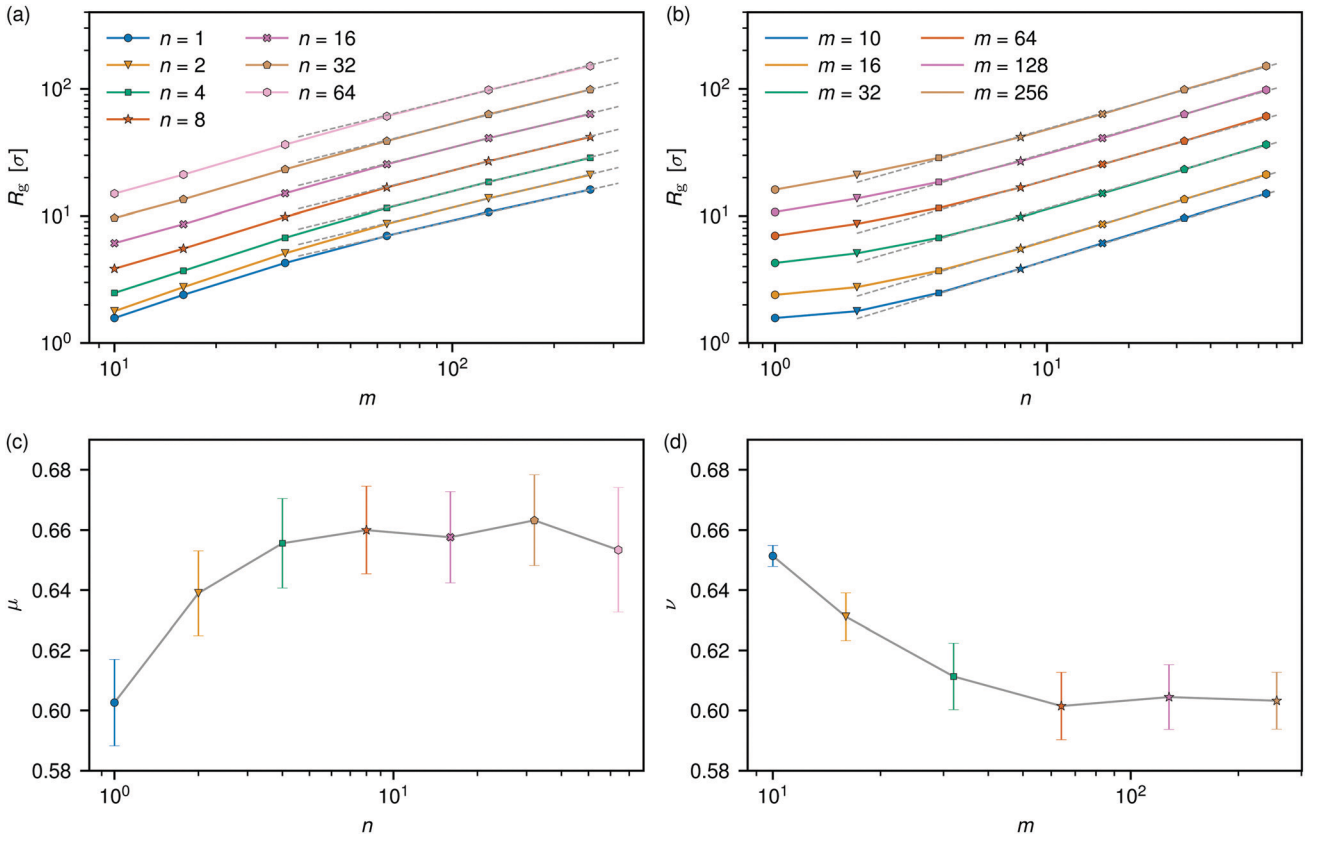

Fig. 2 Scaling of the radius of gyration of semi-flexible ($K_\theta = 4\varepsilon$) poly[n]catenanes. (a) The radius of gyration, R_g, as a function of the macrocycle length m for different numbers of macrocycles n in a poly[n]catenane. The dashed gray lines indicate the scaling $R_g \sim m^\mu$ with the fitted values of μ shown in (c). (b) R_g as a function of n for various m. Here, the dashed gray lines indicate the scaling $R_g \sim n^\nu$ with the fitted values of ν given in (d). In (a) and (b), the error bars are smaller than the symbol sizes.

semi-flexible ring, corresponding to the case with $n = 1$, we obtain $\mu = 0.602 \pm 0.015$ (the error bars here and below are fitting error bars), which is consistent with the value 0.588 known for linear and ring polymers under good solvent conditions.[17] Secondly, for poly[n]catenanes ($n \leq 64$) with macrocycles of size $m = 10$ we observe more swollen conformation characterized by $\nu = 0.651 \pm 0.004$, as compared to fully flexible linear chains of length n in a good solvent. More importantly, we observe an increase in μ upon increasing the number of interlocked rings n in a poly[n]catenane with μ saturating around the value 0.65 ± 0.02, as observed systematically for all $n \geq 2$. In contrast, the ν exponent decays from 0.651 ± 0.004 ($m = 10$) to 0.60 ± 0.01 ($m \geq 64$) with increasing m, that is converging to the value found for linear polymer chains. Thus, given the sample parameters for μ, the value 0.60 lies around two and a half standard deviations below its observed mean 0.65. In addition, we obtained the values $\nu = 0.602 \pm 0.006$ and $\mu = 0.658 \pm 0.010$ by directly performing a non-linear fit with the expression in eqn (6), which is in agreement with the saturation values of the exponents in Fig. 2(c) and (d) calculated separately for different n and m. For the given range of m and n, within statistical precision our results indicate a clear disparity between μ and ν with the value of μ exceeding that of ν by about 10%. Finally, to assess the quality of the fits, we computed the goodness of fit parameter[65] $Q = \Gamma^{-1}(n_{\mathrm{dof}}/2)\int_{\chi^2/2}^{+\infty} t^{n_{\mathrm{dof}}/2-1}\mathrm{e}^{-t}\mathrm{d}t$, where n_{dof} is the number of degrees of freedom in the fit and $\chi^2 = \sum_{i=1}^{N}\left[\left(y_i - y_i^{\mathrm{fitted}}\right)/\sigma_i\right]^2$ (σ_i is the standard deviation for the i-th data point y_i and y_i^{fitted} is the corresponding fitted value). When the initial data points are included in the fit, both for fitting μ and ν, we obtain very small Q values approaching 0, which clearly indicates poor quality of the fit. When using only higher values of n ($n > 8$) and m ($m > 32$), we obtain $Q \approx 0.3$–0.8 for different μ and ν fits (poly[n]catenanes with different n and m), indicating fine quality of the results.

The difference between the values of μ and ν for a poly[n]-catenane can be rationalized in terms of Flory-like arguments that capture essential behavior of polymers in good and athermal solvents. We now assert that the free energy of a poly[n]catenane composed of macrocycles of length m swollen to size R beyond its ideal size can be expressed as:

$$F(R) = F_0(R) + F_{\mathrm{int}}(R), \tag{7}$$

where the first term $F_0(R)$ represents the ideal, reference contribution to the free energy and the second term stands for the energetic contribution coming from monomer–monomer

excluded volume interactions, $F_{\mathrm{int}}(R) \approx k_{\mathrm{B}}T \times v(T)N^2/R^3$, in which $N = n \times m$ and $v(T)$ is the excluded volume of a monomer.

To proceed further, an explicit expression for the reference free energy $F_0(R)$ is required, and due to the presence of topological bonds, expressing it in powers of m and n is not as straightforward as for an ideal linear chain. More specifically, if the excluded volume interactions in a poly[n]catenane were turned off, the topological (or mechanical) bonds within it would break, thereby destroying the peculiar poly[n]catenane's architecture. Therefore, we argue that in the ideal, reference state of a poly[n]catenane it is necessary to explicitly prohibit the bond crossings to maintain the polymer's architecture, albeit omitting at the same time the excluded volume of monomers by assuming, for example, that they are infinitely thin. Furthermore, to avoid unnecessary complications let us additionally assume that each macrocycle within a poly[n]catenane possesses a trivial ring topology with no knots present. As argued by Grosberg[66] and shown by Deutsch[67] in simulations, the size R of an ideal ring polymer subject to topological constraints scales as $R \approx b_0 m^{\nu_0}$ for big enough contour lengths m, that is with ν assuming the good solvent value $\nu_0 = 0.588 \approx 3/5$. Furthermore, the uncrossability conditions between two rings lead to an additional topological excluded volume,[68] $v_{\mathrm{T}} \approx (b_0 m^{\nu_0})^3 = \nu' m^{3\nu_0}$, where each ring has an extent of order $b_0 m^{\nu_0}$ and $\nu' \simeq {b_0}^3$ is a microscopic volume. Thus, the reference term $F_0(R)$ can be written as:

$$F_0(R) \approx k_{\mathrm{B}}T\left(\frac{R^2}{b_0^2 n m^{2\nu_0}} + \nu'\frac{m^{3\nu_0}n^2}{R^3}\right), \tag{8}$$

where the first term $F_{\mathrm{el}} \approx k_{\mathrm{B}}T \times R^2/{R_0}^2$ represents the entropic, elasticity contribution with ${R_0}^1 \approx {b_0}^1 n^{1/2} m^{\nu_0}$ denoting the size of an ideal linear chain of n self-avoiding rings each of length m. The second term $F_{\mathrm{top}} \approx k_{\mathrm{B}}T \times \nu' m^{3\nu_0} n^2/R^3$ accounts for the additional topological exclusion between n rings that are distributed uniformly in a volume R^3, and that each of them topologically excludes for the volume $v_{\mathrm{T}} \approx \nu' m^{3\nu_0}$. Upon minimizing $F_0(R)$, we obtain that $R \sim (nm)^{3/5}$, that is a poly[n]catenane with bond-crossings prohibited is a self-avoiding chain in the number of its monomers $N = nm$.

In order to explicitly include the monomer–monomer excluded volume, we combine eqn (7) and (8) and obtain an augmented Flory free energy of the form:

$$F(R) \approx k_{\mathrm{B}}T\left(\frac{R^2}{{b_0}^2 n m^{2\nu_0}} + \nu'\frac{m^{3\nu_0}n^2}{R^3} + \nu\frac{m^2 n^2}{R^3}\right). \tag{9}$$

A comparison of the powers of m in the second and third terms in eqn (9) reveals that the latter one prevails, since both ν' and ν are constants of order ${b_0}^3$. More specifically, assuming that the second term can be neglected, the size of the poly[n]catenane is obtained as

$$R \sim n^{3/5} m^{2(\nu_0+1)/5} \approx n^{3/5} m^{16/25}, \tag{10}$$

as long as $m^{2-3\nu_0} \approx m^{1/5} \gg |\nu'/\nu| \sim \mathcal{O}(1)$, that is it holds for sufficiently large values of m. As a result, the size of the whole poly[n]catenane scales with the number of rings n as n^{ν} with $\nu \approx 3/5$, as if it was a linear chain of n monomers in a good solvent, whereas its scaling with m features a somewhat higher value of the exponent $\mu \approx 16/25 = 0.64$. As seen from Fig. 2(c) and (d), these values for the exponents are in agreement with our simulation results within the error bars.

In addition, the studies of Grosberg[66] and Deutsch[67] also show that topological constraints have a negligible effect on shorter rings, which scale as $m^{1/2}$ with their contour length m ($m \lesssim 32$ according to ref. 67). For poly[n]catenanes this scaling would imply that ${R_0}^2 \approx {b_0}^2 mn$ in the reference free energy (8), leading to $R \approx b_0(mn)^{\nu_0}$ with $\nu_0 \approx 3/5$ obtained by minimization, that is with $\mu = \nu$. Interestingly, this expression is consistent with the results of Pakula and Jeszka,[51] who simulated poly[n]catenanes consisting of relatively short rings on a lattice, and found with good precision that $R_{\mathrm{g}} \sim (mn)^{3/5}$. In our case, however, we do not observe such regime for poly[n]catenanes with short rings, highly likely because of the bending rigidity that dominates conformations of rings with small m.

4 Worsening solvent quality

The Flory arguments outlined in the previous section explicitly rely on the fact that within an ideal poly[n]catenane individual macrocycles are self-avoiding. In practice, ideal conformations are reached through a balance between excluded volume and attractions, at the θ-point of the macromolecule. The issue therefore is whether the θ-point of the whole poly[n]catenane coincides with that of the macrocycle that constitutes the "macromonomer" of the former. In this section, we set out to explicitly verify this by examining the effects of worsening solvent quality on poly[n]catenanes. To focus solely on the influence of topological bonds, here we consider fully flexible polymer chains, that is with $K_\theta = 0$ in the bending potential (3). The gradual worsening of solvent quality is achieved by increasing the attraction parameter λ, which denotes the depth of the Lennard-Jones excluded volume potential (1).

To determine the θ-point of any sequentially connected polymer composed of $\mathcal{N}$ units, we make use of the fact that under θ-conditions it exhibits random-walk behavior, which results in the scaling of its size $\mathcal{R}$ with $\mathcal{N}$ as:

$$\mathcal{R} \sim \mathcal{N}^{1/2}. \tag{11}$$

The equation above offers a straightforward way of determining the θ-temperature computationally by simulating a few polymers of different lengths $\mathcal{N}$ (big enough polymers should be used to assure that the scaling limit of the employed model is close) at different values of the attraction parameter λ. Then, the θ-point, if it exists, will correspond to the intersection point of the curves $\mathcal{R}/\sqrt{\mathcal{N}}$ plotted *versus* λ. Furthermore, for ring polymers with a fixed topological state, which form the building blocks of poly[n]catenanes, it has been shown by Narros *et al.*[17] that the Gaussianity of conformations practically coincides with the point at which the second virial coefficient of the interaction between two ring polymers vanishes. Recent studies of the relationship between conformations and interactions in the systems of ring polymers under varying solvent

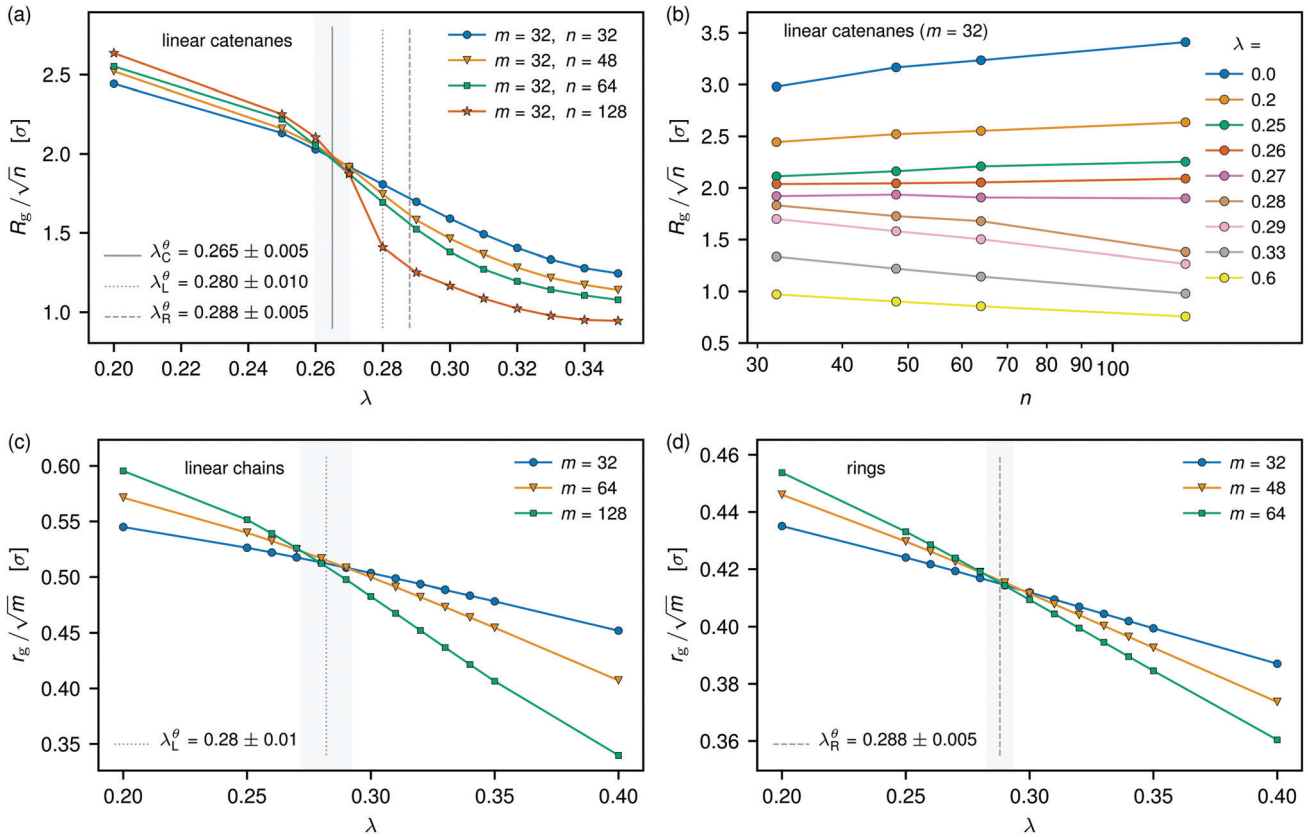

Fig. 3 Influence of molecular architecture on the location of the θ-point. The radius of gyration, R_g, of a linear catenane composed of n interlinked ring polymers of length $m = 32$ and scaled over $\sqrt{n}$ as a function of (a) λ for different n and (b) n for different λ, values of which are indicated in the legend. The radius of gyration, r_g, of (c) linear and (d) ring polymers of different length m scaled over $\sqrt{m}$ as a function of λ. In (a), the gray solid, dotted, and dashed line indicate the location of the θ-temperature of the linear catenane ($\lambda_C^\theta = 0.265 \pm 0.005$), linear chain ($\lambda_L^\theta = 0.28 \pm 0.01$), and ring ($\lambda_R^\theta = 0.288 \pm 0.005$), respectively, as determined by the condition (11) (the shaded area around vertical lines corresponds to the uncertainty regions for each determined θ-point). Error bars of each data point are in general comparable with its symbol size.

conditions have also been carried out by Li *et al.*[69] and by Gartner *et al.*[70]

We determined the θ-point of a fully flexible poly[n]catenane composed of macrocycles of size $m = 32$ by simulating catenane chains with different numbers of macrocycles n ($n = 32$, 48, 64 and 128) for different λ and then finding the intersection point between the curves $R_g(\lambda;n)/\sqrt{n}$, as shown in Fig. 3(a). All four lines intersect in a very narrow region of λ, indicating that the θ-point of the poly[n]catenane is located close to $\lambda_C^\theta = 0.265 \pm 0.005$. To further support this, in Fig. 3(b) we plot $R_g/\sqrt{n}$ as a function of n for different values of λ, resulting in almost flat curves around $\lambda = 0.26$. In addition, to compare with the latter result we determined the θ-temperatures of linear and ring polymers, yielding the values $\lambda_L^\theta = 0.28 \pm 0.01$ and $\lambda_R^\theta = 0.288 \pm 0.005$, respectively. In agreement with ref. 17, we obtained that ring polymers feature a lower, although by a small amount, θ-temperature than linear chains (note that temperature is inversely proportional to λ). Interestingly, the poly[n]catenane possesses a higher θ-temperature in comparison to both linear and ring polymers with the relative difference amounting to approximately $1 - T_L^\theta/T_C^\theta = 1 - \lambda_C^\theta/\lambda_L^\theta \approx 5\%$ in temperature for the former case. As each macrocycle within a catenane is pierced by two (or by one at the ends) other macrocycles, such piercings effectively act as additional attraction spots within the backbone as the solvent quality is being worsened. Moreover, each ring experiences surplus pressure due to topological interaction with other rings. Apparently, both effects in conjunction make it easier for a poly[n]catenane to collapse, if additional attraction between its monomers is introduced, and consequently leads to heightening of its θ-temperature.

In retrospect, this also offers additional confirmation of the Flory argument presented above, now applied to real monomers with excluded volume and attractions: as the temperature is lowered and the θ-point of the poly[n]catenane is reached, at which the latter features ideal, $R_g \sim n^{1/2}$ scaling, its constituent macrocycles are still scaling as self-avoiding walks, $r_g \sim m^{\nu_0}$.

5 Effect of linking on the ring's size and θ-temperature

Based on the above findings that underline the effect of topological constraints on polymer sizes and scaling, we now investigate in more detail the effect of linking on the size and θ-temperature of a ring polymer within catenanes.

First of all, we report that r_g of a ring polymer within a catenane (either a poly[n]catenane or a star-shaped one) depends neither on the catenane's architecture, nor on the absolute location of the macrocycle within it, but only on the number of other rings N_L to which the given one is linked. In Fig. 4(a), we show the radius of gyration of semiflexible ring polymers with N_L = 0, 1, 2 under good solvent conditions, obtained from the simulations of poly[n]catenanes with the same n and m as the ones used in Section 3 (for a fixed m, the statistics were gathered over all corresponding macrocycles in poly[n]catenanes of every length n considered). We observe that the presence of a link increases the size of a ring with r_g of the latter monotonically rising with N_L (for example, the rings with N_L = 2 are swollen by about 10% in comparison to the ones with N_L = 0, as seen in the inset of Fig. 4(a)). However, the linking does not affect the scaling of the single ring's size with its polymerization degree m and the measured exponent approaches 0.60 ± 0.01 for longer rings. Furthermore, for small m = 10 and m = 16 whose length is of the order of the macrocycle's Kuhn length ($l_k \approx 8\sigma$) the swelling ratio due to a link, defined as $r_g(N_L)/r_g(N_L = 0)$, slightly increases with N_L. We note that this enhancement rises with the macrocycle's size m and for the units that are long enough compared to the Kuhn length this ratio appears to approach a universal form as can be seen in the inset of Fig. 4(a) for m = 128 and 256. Therefore, we conjecture that r_g of a linked ring in a good solvent can be written as $r_g(N_L,m) \sim \eta(N_L)m^{\nu}$, where $\eta(N_L)$ is a universal function. To support this hypothesis, we simulated relatively short fully flexible rings (K_θ = 0 in eqn (3)) with m = 32, 48, and 64 for higher values of N_L (up to N_L = 5) in star-shaped catenane structures in good solvents (λ = 0 in eqn (1)). The gyration radii of fully flexible rings as well as the corresponding swelling ratios $r_g(N_L)/r_g(N_L = 0)$ are shown in Fig. 4(b). For every m considered, we observe almost identical forms of the swelling parameter, as shown in the inset of Fig. 4(b). The swelling ratio increases with N_L, with its derivative decreasing at the same time, meaning that the successive addition of each link increases the size of a ring less than the addition of the previous one, indicating that $\eta(N_L)$ might saturate at a constant value for a high number of links. These results suggest that $\eta(N_L)$ is indeed a universal function for linked rings under good solvent conditions, however a more thorough study of catenane structures featuring higher N_L is necessary to determine its actual functional form. Finally, coming back to the obtained scaling relation (10) for the poly[n]catenane, we see that although the macrocycle itself in the catenane scales as $r_g \sim b_0 m^{\nu_0} = b_0 m^{3/5}$, the whole macromolecule (*i.e.*, the polycatenane) does not simply scale as $R \sim r_g n^{\nu}$, which would imply that eqn (5) holds instead of eqn (10). The answer is that the correct scaling is, of course, $R \sim \langle b_m \rangle n^{\nu}$, where $\langle b_m \rangle$ is the expectation value of the effective bond distance between two successive, linked macrocycles. There is no *a priori* reason to expect that this will scale the same way as the r_g of the macrocycle in the catenane. Due to the additional topological repulsions caused by the mutually penetrating/linked strands of the successive macrocycles, the average bond length scales as $\langle b_m \rangle \sim m^{\mu}$ with μ = 16/25, resulting in the anomalous exponent of the overall scaling of the polycatenane.

We finally turn our attention to the effect of linking on the θ-temperature of a ring polymer *within* an [n]catenane. To determine the θ-points, we simulated a fully flexible star-shaped [7]catenane, composed of three arms, each consisting of two macrocycles interlinked with a common central ring. Therefore, this structure contained one ring with N_L = 3, three rings in the interior with N_L = 2, and three rings at the end of each arm with N_L = 1. As other rings linked to a given one impose additional uncrossability constraints, they can be effectively treated as fluctuating poles that topologically restrict the phase space of the central ring. Upon worsening the solvent conditions, the piercing rings, depending on the interactions with the central ring, can either (a) serve as additional attraction centers (if all interactions are attractive), which is beneficial for the collapse of the central, pierced ring, or (b) oppose the collapse (if cross interactions as well as interactions between piercing rings are repulsive). Therefore, to distinguish these two cases and to

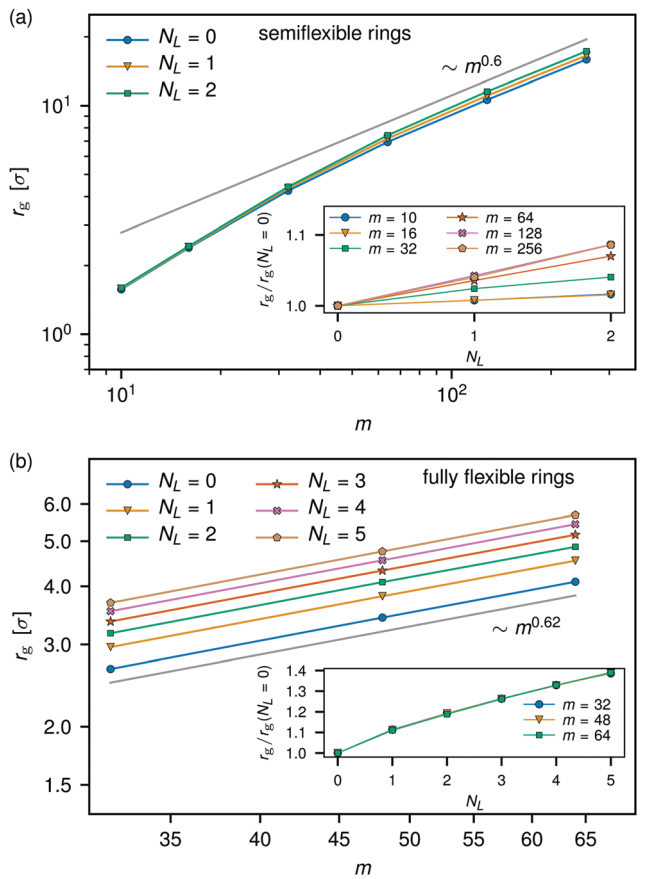

Fig. 4 Influence of linking on the radius of gyration of individual ring polymers within a catenane. The radius of gyration r_g of semiflexible (a) and fully flexible (b) rings interlocked with different numbers of other rings of the same type N_L plotted *versus* their polymerization degree m on a log–log scale. The solid gray lines in (a) and (b) indicate the scaling behavior $r_g \sim m^{\nu}$ with $\nu_{\text{semiflexible}}$ = 0.60 ± 0.01 and ν_{flexible} = 0.62 ± 0.01 obtained for the values of m considered. Insets: The swelling ratio $r_g(N_L)/r_g(N_L = 0)$ of linked rings as a function of N_L. In each case, error bars are smaller than the corresponding symbol sizes.

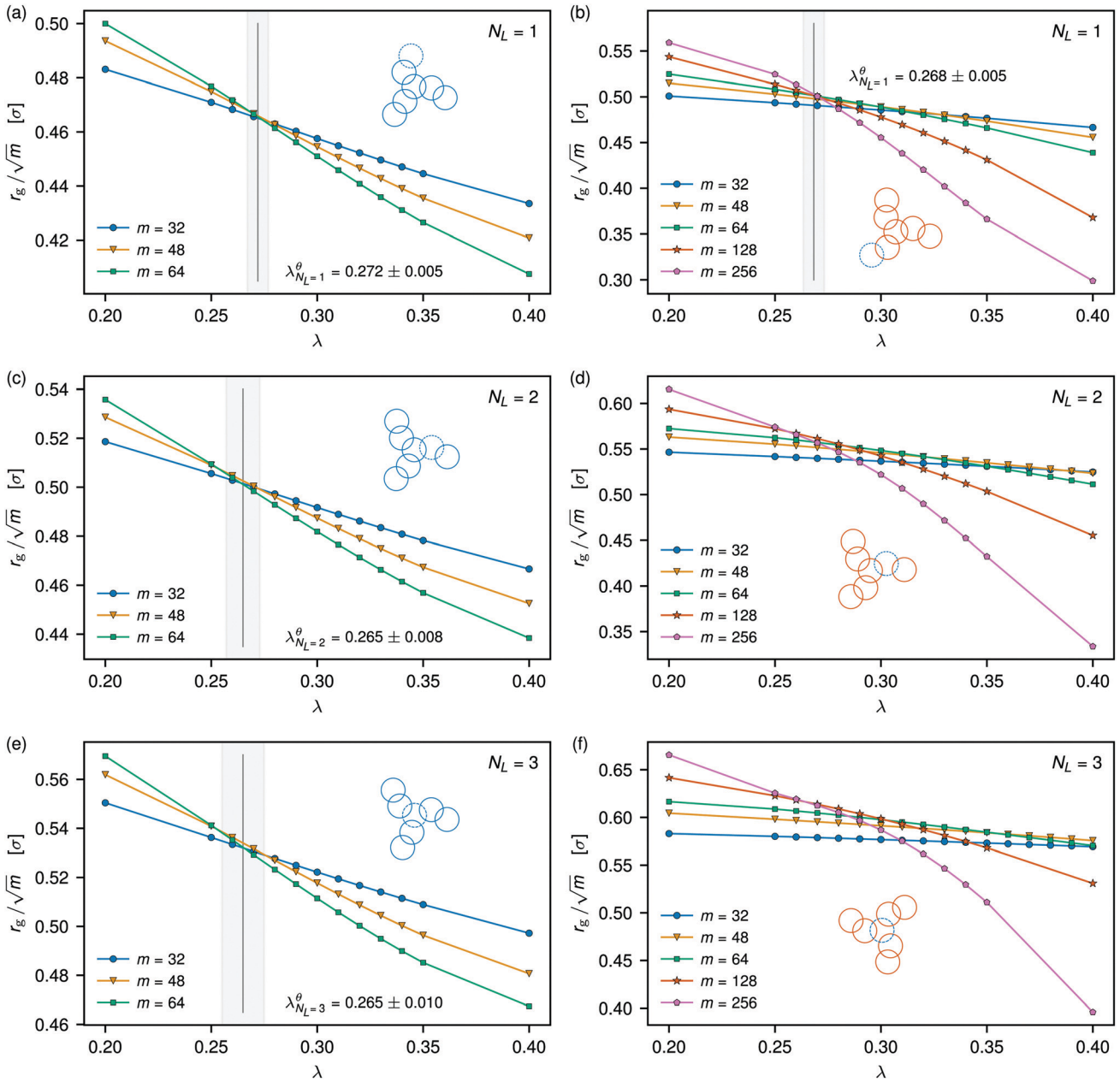

Fig. 5 Determining the θ-temperature of a linked ring polymer in a star-shaped [7]catenane. Left column: interactions among all monomers are attractive as indicated by the blue color on the sketches in the insets. Right columns: interactions only among the monomers within a single macrocycle are attractive, whereas all other interactions are fully repulsive as indicated by the red color on the sketches in the insets. Rings for which the statistics was sampled are indicated by dashed lines. The radius of gyration of a ring polymer r_g scaled over $\sqrt{m}$ as a function of the attraction parameter λ for N_L = 1 (top row), 2 (middle row), and 3 (bottom row) for both systems. For the first system, the θ-point for each N_L lies very close to the one of a poly[n]catenane λ^{θ}_{C} = 0.265 ± 0.005 (the solid gray lines in (a), (c), and (e)). For the second system, we were able to define a θ-point only for the case with N_L = 1 using three biggest m = 64, 128, and 256 considered, resulting in $\lambda^{\theta}_{N_L=1} = 0.268 + 0.005$ (the solid gray line in (b)). No such points can be defined for panels (d) and (f).

study the effect of such potentially different interactions on the θ-point of a linked ring, we considered two distinct models: (1) in the first one (left column of Fig. 5), interactions among all monomers are attractive (that is, the same λ); (2) in the second one (right column of Fig. 5), interactions only among the monomers within a target macrocycle are attractive with a given λ, whereas interactions among all other monomers as well as the cross interactions are completely repulsive (λ = 0). Accordingly, we simulated the same structure for different lengths m of the constituting macrocycles to determine the θ-point using the procedure outlined in Section 4 and the results are as follows. For the first model (see Fig. 5(a), (c), and (e)), we were able to define a θ-point for each fixed number of links N_L, with the resulting values being very close to each other and approaching the one of a poly[n]catenane λ^{θ}_{C} = 0.265 ± 0.005. In the other case (see Fig. 5(c), (d), and (f)), we found a θ-point only

for the case with $N_L = 1$, although considering only rings of bigger size ($m = 64$, 128 and 256), giving the value $\lambda^{\theta}_{N_L=1} = 0.268 + 0.005$, which is also very close to the one of the poly[n]catenane. For $N_L = 2$ and $N_L = 3$ we did not find a common intersection between three successive ring lengths even for m = 64, 128 and 256, however it might still be possible to define the θ-point when much longer rings are considered, that is when two-body contacts imposed by the topological bonds become less pronounced. Here, the effects of the neighboring rings that have pure, repulsive interactions with the target one and exert on it additional osmotic pressure from the exterior are crucial and they lead to a lack of intersection of all curves at a common point.

6 Conclusions

We have studied the effects of topological (mechanical) bonds on the size of poly[n]catenanes in a good solvent as well as on its θ-temperature upon worsening the solvent quality. Employing Flory-like arguments, we have shown that in a good solvent the size of a poly[n]catenane can be expressed as $R_g \sim m^{\mu}n^{\nu}$ where n is the number of macrocycles in the catenane, m is the size of a macrocycle, and $\mu \approx 16/25$ and $\nu \approx 3/5$. In our simulations of semiflexible poly[n]catenanes, we have found a discrepancy between the two exponents, yielding values of μ and ν comparable with those predicted by the Flory theory. Furthermore, our results indicate that the size of a ring polymer of length m interlocked with N_L other rings in a good solvent can be expressed as $r_g \sim \eta(N_L)m^{\nu}$ ($\nu \approx 3/5$) with $\eta(N_L)$ being a universal monotonically rising function of N_L. We have studied the influence of topological bonds on the θ-temperature of poly[n]catenanes that has been found to be about 5% higher than the one of ordinary linear chains. Moreover, we have found that $T^{\theta}_{\text{catenane}} > T^{\theta}_{\text{linear}} > T^{\theta}_{\text{ring}}$. Finally, we have shown that similar heightening of the θ-temperature occurs if individual ring polymers are interlocked with other rings, and we have found that the resulting θ-temperature of linked rings is very close to the one of poly[n]catenanes.

Conflicts of interest

There are no conflicts to declare.

Acknowledgements

Z. A. D. would like to thank the IPM institute for their hospitality and the University of Vienna for hospitality and providing computational resources, and the Erwin Schrödinger Institute for Mathematics and Physics (Vienna) for providing financial support. Computational time at the Vienna Scientific Cluster (VSC) is gratefully acknowledged.

Notes and references

1 M. D. Frank-Kamenetskii, A. V. Lukashin and A. V. Vologodskii, *Nature*, 1975, **258**, 398–402.
2 D. Marenduzzo and E. Orlandini, *J. Stat. Mech.: Theory Exp.*, 2009, L09002.
3 M. Bohn and D. W. Heermann, *J. Chem. Phys.*, 2010, **132**, 044904.
4 A. Narros, A. J. Moreno and C. N. Likos, *Soft Matter*, 2010, **6**, 2435–2441.
5 A. Narros, A. J. Moreno and C. N. Likos, *Macromolecules*, 2013, **46**, 9437–9445.
6 A. Narros, A. J. Moreno and C. N. Likos, *Biochem. Soc. Trans.*, 2013, **41**, 630–634.
7 M. Kapnistos, M. Lang, D. Vlassopoulos, W. Pyckhout-Hintzen, D. Richter, D. Cho, T. Chang and M. Rubinstein, *Nat. Mater.*, 2008, **7**, 997.
8 J. D. Halverson, J. Smrek, K. Kremer and A. Y. Grosberg, *Rep. Prog. Phys.*, 2014, **77**, 022601.
9 J. D. Halverson, W. B. Lee, G. S. Grest, A. Y. Grosberg and K. Kremer, *J. Chem. Phys.*, 2011, **134**, 204904.
10 J. D. Halverson, W. B. Lee, G. S. Grest, A. Y. Grosberg and K. Kremer, *J. Chem. Phys.*, 2011, **134**, 204905.
11 D. Michieletto, N. Nahali and A. Rosa, *Phys. Rev. Lett.*, 2017, **119**, 197801.
12 D. Michieletto and M. S. Turner, *Proc. Natl. Acad. Sci. U. S. A.*, 2016, **113**, 5195–5200.
13 J. Smrek, K. Kremer and A. Rosa, *ACS Macro Lett.*, 2019, **8**, 155–160.
14 J. Smrek and A. Y. Grosberg, *ACS Macro Lett.*, 2016, **5**, 750–754.
15 J. Smrek, I. Chubak, C. N. Likos and K. Kremer, *Nat. Commun.*, 2020, **11**, 26.
16 S. S. Jang, T. Çağin and W. A. Goddard, *J. Chem. Phys.*, 2003, **119**, 1843–1854.
17 A. Narros, A. J. Moreno and C. N. Likos, *Macromolecules*, 2013, **46**, 3654–3668.
18 C. Micheletti and E. Orlandini, *Macromolecules*, 2012, **45**, 2113–2121.
19 I. Chubak, E. Locatelli and C. N. Likos, *Mol. Phys.*, 2018, **116**, 2911–2926.
20 M. Liebetreu, M. Ripoll and C. N. Likos, *ACS Macro Lett.*, 2018, **7**, 447–452.
21 L. B. Weiss, A. Nikoubashman and C. N. Likos, *ACS Macro Lett.*, 2017, **6**, 1426–1431.
22 L. B. Weiss, M. Marenda, C. Micheletti and C. N. Likos, *Macromolecules*, 2019, **52**, 4111–4119.
23 H. Salari, B. Eslami-Mossallam, H. F. Ranjbar and M. R. Ejtehadi, *Phys. Rev. E*, 2016, **94**, 062407.
24 A. Fathizadeh, B. Eslami-Mossallam and M. R. Ejtehadi, *Phys. Rev. E: Stat., Nonlinear, Soft Matter Phys.*, 2012, **86**, 051907.
25 B. Eslami-Mossallam and M. R. Ejtehadi, *J. Chem. Phys.*, 2008, **128**, 125106.
26 H. Salari, B. Eslami-Mossallam, S. Naderi and M. R. Ejtehadi, *J. Chem. Phys.*, 2015, **143**, 104904.
27 Q. Du, C. Smith, N. Shiffeldrim, M. Vologodskaia and A. Vologodskii, *Proc. Natl. Acad. Sci. U. S. A.*, 2005, **102**, 5397–5402.
28 A. Fathizadeh, H. Schiessel and M. R. Ejtehadi, *Macromolecules*, 2015, **48**, 164–172.
29 C. J. Dorman, *BMC Mol. Cell Biol.*, 2019, **20**, 2661–8850.
30 Z. Niu and H. W. Gibson, *Chem. Rev.*, 2009, **109**, 6024–6046.

31 E. Wasserman, *J. Am. Chem. Soc.*, 1960, **82**, 4433–4434.
32 C. Dietrich-Buchecker and J.-P. Sauvage, *Tetrahedron*, 1990, **46**, 503–512.
33 Q. Wu, P. M. Rauscher, X. Lang, R. J. Wojtecki, J. J. de Pablo, M. J. A. Hore and S. J. Rowan, *Science*, 2017, **358**, 1434–1439.
34 B. Hudson and J. Vinograd, *Nature*, 1967, **216**, 647–652.
35 S. Wasserman and N. Cozzarelli, *Science*, 1986, **232**, 951–960.
36 S. Erbas-Cakmak, D. A. Leigh, C. T. McTernan and A. L. Nussbaumer, *Chem. Rev.*, 2015, **115**, 10081–10206.
37 K. K. Cotí, M. E. Belowich, M. Liong, M. W. Ambrogio, Y. A. Lau, H. A. Khatib, J. I. Zink, N. M. Khashab and J. F. Stoddart, *Nanoscale*, 2009, **1**, 16–39.
38 G. Gil-Ramírez, D. A. Leigh and A. J. Stephens, *Angew. Chem., Int. Ed.*, 2015, **54**, 6110–6150.
39 J. Chen, C. A. Rauch, J. G. White, P. T. Englund and N. R. Cozzarelli, *Cell*, 1995, **80**, 61–69.
40 Y. Diao, K. Hinson, Y. Sun and J. Arsuaga, *J. Phys. A: Math. Theor.*, 2015, **48**, 435202.
41 M. Lang, J. Fischer, M. Werner and J.-U. Sommer, *Phys. Rev. Lett.*, 2014, **112**, 238001.
42 J. Fischer, M. Lang and J.-U. Sommer, *J. Chem. Phys.*, 2015, **143**, 243114.
43 A. Van Quaethem, P. Lussis, D. A. Leigh, A.-S. Duwez and C.-A. Fustin, *Chem. Sci.*, 2014, **5**, 1449–1452.
44 B. Nisar Ahamed, R. Duchêne, K. Robeyns and C.-A. Fustin, *Chem. Commun.*, 2016, **52**, 2149–2152.
45 J.-L. Weidmann, J.-M. Kern, J.-P. Sauvage, D. Muscat, S. Mullins, W. Köhler, C. Rosenauer, H. J. Räder, K. Martin and Y. Geerts, *Chem. – Eur. J.*, 1999, **5**, 1841–1851.
46 Z. Xiong, C. C. Han and Q. Liao, *J. Chem. Phys.*, 2012, **136**, 134902.
47 A. Vologodskii and V. V. Rybenkov, *Phys. Chem. Chem. Phys.*, 2009, **11**, 10543–10552.
48 G. D'Adamo, E. Orlandini and C. Micheletti, *Macromolecules*, 2017, **50**, 1713–1718.
49 E. Orlandini, G. Polles, D. Marenduzzo and C. Micheletti, *J. Stat. Mech.: Theory Exp.*, 2017, 034003.
50 M. Caraglio, C. Micheletti and E. Orlandini, *Polymers*, 2017, **9**, 327.
51 T. Pakula and K. Jeszka, *Macromolecules*, 1999, **32**, 6821–6830.
52 S. Natori and H. Takano, *J. Phys. Soc. Jpn.*, 2017, **86**, 043003.
53 P. M. Rauscher, S. J. Rowan and J. J. de Pablo, *ACS Macro Lett.*, 2018, **7**, 938–943.
54 Y. Weizmann, A. B. Braunschweig, O. I. Wilner, Z. Cheglakov and I. Willner, *Proc. Natl. Acad. Sci. U. S. A.*, 2008, **105**, 5289–5294.
55 F. L. T. Li and M. Famulok, *Nat. Commun.*, 2014, **5**, 4940.
56 C.-H. Lu, A. Cecconello, X.-J. Qi, N. Wu, S.-S. Jester, M. Famulok, M. Matthies, T.-L. Schmidt and I. Willner, *Nano Lett.*, 2015, **15**, 7133–7137.
57 T. Li, H. Zhang, L. Hu and F. Shao, *Bioconjugate Chem.*, 2016, **27**, 616–620.
58 C.-H. Lu, A. Cecconello and I. Willner, *J. Am. Chem. Soc.*, 2016, **138**, 5172–5185.
59 M. Rubinstein and R. H. Colby, *Polymer Physics*, Oxford University Press, New York, 2003.
60 S. Huissmann, R. Blaak and C. N. Likos, *Macromolecules*, 2009, **42**, 2806–2816.
61 S. Plimpton, *J. Comput. Phys.*, 1995, **117**, 1–19.
62 J. A. Anderson, C. D. Lorenz and A. Travesset, *J. Comput. Phys.*, 2008, **227**, 5342–5359.
63 J. Glaser, T. D. Nguyen, J. A. Anderson, P. Lui, F. Spiga, J. A. Millan, D. C. Morse and S. C. Glotzer, *Comput. Phys. Commun.*, 2015, **192**, 97–107.
64 M. P. Howard, J. A. Anderson, A. Nikoubashman, S. C. Glotzer and A. Z. Panagiotopoulos, *Comput. Phys. Commun.*, 2016, **203**, 45–52.
65 W. H. Press, S. A. Teukolsky, W. T. Vetterling and B. P. Flannery, *Numerical Recipes 3rd Edition: The Art of Scientific Computing*, Cambridge University Press, USA, 3rd edn, 2007.
66 A. Y. Grosberg, *Phys. Rev. Lett.*, 2000, **85**, 3858–3861.
67 J. M. Deutsch, *Phys. Rev. E*, 1999, **59**, R2539–R2541.
68 J. Des Cloizeaux, *J. Phys. Lett.*, 1981, **42**, 433–436.
69 B. Li, Z. Sun, L. An and Z.-G. Wang, *Sci. China: Chem.*, 2016, **59**, 619–623.
70 T. E. Gartner, F. M. Haque, A. M. Gomi, S. M. Grayson, M. J. A. Hore and A. Jayaraman, *Macromolecules*, 2019, **52**, 4579–4589.

